Photocatalytic properties of h-WO3 nanoparticles obtained by annealing and h-WO3 nanorods prepared by hydrothermal method

Stefan I. Boyadjiev, Teodóra Nagy-Kovács, István Lukács, and Imre M. Szilágyi

Citation: AIP Conference Proceedings **1722**, 140003 (2016); doi: 10.1063/1.4944193
View online: http://dx.doi.org/10.1063/1.4944193
View Table of Contents: http://scitation.aip.org/content/aip/proceeding/aipcp/1722?ver=pdfcov
Published by the AIP Publishing

Photocatalytic properties of h-WO_3 nanoparticles obtained by annealing and h-WO_3 nanorods prepared by hydrothermal method

Stefan I. Boyadjiev[1, a)], Teodóra Nagy-Kovács[2], István Lukács[3] and Imre M. Szilágyi[1, 2, b)]

[1]*MTA-BME Technical Analytical Chemistry Research Group, Szent Gellért tér 4, Budapest, H-1111, Hungary.*
[2]*Budapest University of Technology and Economics, Department of Inorganic and Analytical Chemistry, Szent Gellért tér 4, Budapest, H-1111, Hungary.*
[3]*Hungarian Academy of Sciences, Research Centre for Energy, Institute of Technical Physics and Materials Science, H-1121 Budapest, Konkoly Thege M. út 29-33, Hungary.*

[a)]*Corresponding author: boiajiev@gmail.com*
[b)]*imre.szilagyi@mail.bme.hu*

Abstract. In the present study, two different methods for preparing hexagonal WO_3 (h-WO_3) photocatalysts were used - controlled thermal decomposition and hydrothermal synthesis. WO_3 nanoparticles with hexagonal structure were obtained by annealing $(NH_4)_xWO_{3-y}$ at 500 °C in air. WO_3 nanorods were prepared by a hydrothermal method using sodium tungstate Na_2WO_4, HCl, $(COOH)_2$ and $NaSO_4$ precursors at 200 °C. The formation, morphology, structure and composition of the as-prepared nanoparticles and nanorods were studied by powder X-ray diffraction (XRD), transmission electron microscopy (TEM), and scanning electron microscopy combined with energy-dispersive X-ray spectroscopy (SEM-EDX). The photocatalytic activity of the h-WO_3 nanoparticles and nanorods was studied by decomposing methyl orange in aqueous solution under UV light irradiation.

INTRODUCTION

WO_3 is an n-type semiconductor with a bandgap of 2.4-2.8 eV and it is one of the most widely researched photocatalysts [1-2]. Its photo-generated h^+ is oxidant enough to generate $^{\bullet}OH$ from water, but the photo-excited e^- cannot reduce the O_2, which decreases its photocatalytic activity. Nevertheless, this is compensated by that WO_3 absorbs also visible light in the most intensive part of the solar spectrum, besides UV light [3-4].

WO_3 has several crystalline modifications, however up to now almost only the monoclinic WO_3 (m-WO_3) was studied as a photocatalysts [5-7]. However, there has been only one study on the photocatalytic properties of the hexagonal WO_3 (h-WO_3) [4]. The h-WO_3 has a three dimensional channel-system along its structure, which is stabilized by cationic impurities, e.g. Li^+, Na^+, K^+, NH_4^+ [8]. Due to this the W atoms in h-WO_3 are partially reduced to maintain electroneutrality, and they can serve as recombination centers during photocatalysis, and decrease the activity. The m-WO_3, on the other hand, is completely oxidized, and therefore has a better photocatalytic activity [4]. Still, the h-WO_3 could be also applied for photocatalysis, especially when its surface is nanostructured and with high surface area.

In order to enhance the photocatalytic efficiency, the catalyst should have high specific surface area. Therefore, in the recent years the researchers are focused on studying novel nanomaterials, like nanoparticles [4,9], nanofibers [10-11], nanorods [12-13], which possess high surface-to-volume ratio, and thus increased photocatalytic effect.

The h-WO_3 sample used for photocatalysis was prepared by annealing hexagonal ammonium tungsten bronze, $(NH_4)_xWO_{3-y}$ (HATB) in air at 500 °C, and was composed of 50-70 nm particles [4]. On the other hand, the hydrothermal synthesis is powerful method for preparing nanostructured WO_3 photocatalysts [13-15]. When SO_4^{2-} is

9th International Physics Conference of the Balkan Physical Union (BPU-9)
AIP Conf. Proc. 1722, 140003-1–140003-4; doi: 10.1063/1.4944193

added to the standard Na_2SO_4 and HCl reaction mixture, it acts as a structure directing agent during the hydrothermal synthesis to obtain h-WO_3 nanorods [16].

Hence, in this study we prepared h-WO_3 nanoparticles by annealing $(NH_4)_xWO_{3-y}$ and h-WO_3 nanorods hydrothermally using Na_2WO_4, HCl, $(COOH)_2$ and $NaSO_4$ as precursors. The as-obtained samples were investigated by powder X-ray diffraction (XRD), transmission electron microscopy (TEM), and scanning electron microscopy combined with energy-dispersive X-ray spectroscopy (SEM-EDX). The photocatalytic activity of the h-WO_3 nanoparticles and nanorods was studied by decomposing methyl orange in aqueous solution under UV light irradiation.

EXPERIMENTAL

Hexagonal WO_3 nanoparticles were prepared by annealing hexagonal ammonium tungsten bronze, $(NH_4)_xWO_{3-y}$, in air at 500 °C. $(NH_4)_xWO_{3-y}$ was prepared by the partial reduction of ammonium paratungstate tetrahydrate, $(NH_4)_{10}[H_2W_{12}O_{42}].4H_2O$ (APT), in H_2 for 6 h at 400 °C [17]. The annealing parameters of $(NH_4)_xWO_{3-y}$ were determined previously to obtain h-WO_3 [18]. At temperatures below 500-550 °C WO_3 crystallizes in the hexagonal structure, while over 550 °C predominantly in the monoclinic structure [19].

Hexagonal WO_3 nanorods were obtained by adding 4.1 g $Na_2WO_4 \cdot 2\ H_2O$ to 100 ml water, then the pH was set to 1 by adding 3 M HCl. Afterwards 3.2 g oxalic acid was added to the solution, and then 60 ml of the solution was poured into a Teflon lined stainless steel autoclave (Parr Instrument, 302 AC T304). It was heated to 200 °C with 1 °C/min and kept there for 24 h. After the reaction, the product was centrifuged and washed with both H_2O and EtOH several times, and dried in air at 60 °C.

The XRD patterns of the samples were recorded by a PANalytical X'pert Pro MPD X-ray diffractometer using Cu Kα radiation. Transmission electron microscopy (TEM) images were taken by an FEI Morgagni 268D device. A JEOL JSM 5500 lv scanning electron microscope (SEM) was used for the SEM-EDX study.

The photocatalytic efficiencies of the as-prepared catalysts were tested in the photo-bleaching reaction of methyl-orange (MO) by UV light (2 parallel 18 W Osram black lights). 1 mg of WO_3 powder was placed inside a quartz cuvette, then 3 mL MO solution (0.0133 mg/ml) was pipetted into the cuvette. It was then closed with Parafilm and left in the dark for 15-30 min, so that the particles can absorb the dye, and an equilibrium can be reached. Methyl orange was selected as a probe molecule, as its absorption maximum (465 nm) is exactly where WO_3 has a minimum in its UV-Vis spectrum. MO is one of the most widespread dyes for testing the photocatalytic activity of WO_3 [14]. Then the lamp was switched on and the decline of the MO concentration was followed by a Jasco V-550 type UV-Vis spectrophotometer.

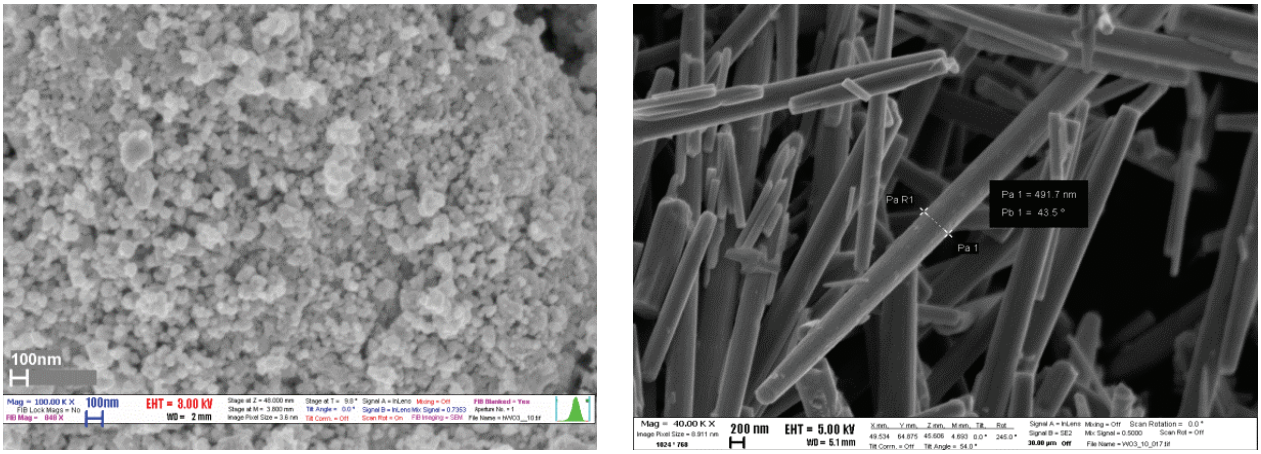

(a) (b)

FIGURE 1. SEM images of h-WO_3 (a) nanoparticles and (b) nanorods.

RESULTS AND DISCUSSION

The morphology of the as-prepared WO_3 samples was studied by SEM (Fig. 1) and TEM (Fig. 2). The h-WO_3 nanoparticles consisted of 50-70 nm particles. While the h-WO_3 nanorods were 5-10 μm long and 150-500 nm thick. Both structures are beneficial for photocatalysis. The EDX study detected the presence of W and O in the h-WO_3 nanoparticles. Nitrogen from NH_4^+ was not observed clearly, since it was present in small amounts [4], and below the detection limit of EDX. In the h-WO_3 nanorods ca. 0.7 m% Na was detected and it was explained by the presence of structure stabilizing Na^+ ions in the hexagonal channels of h-WO_3.

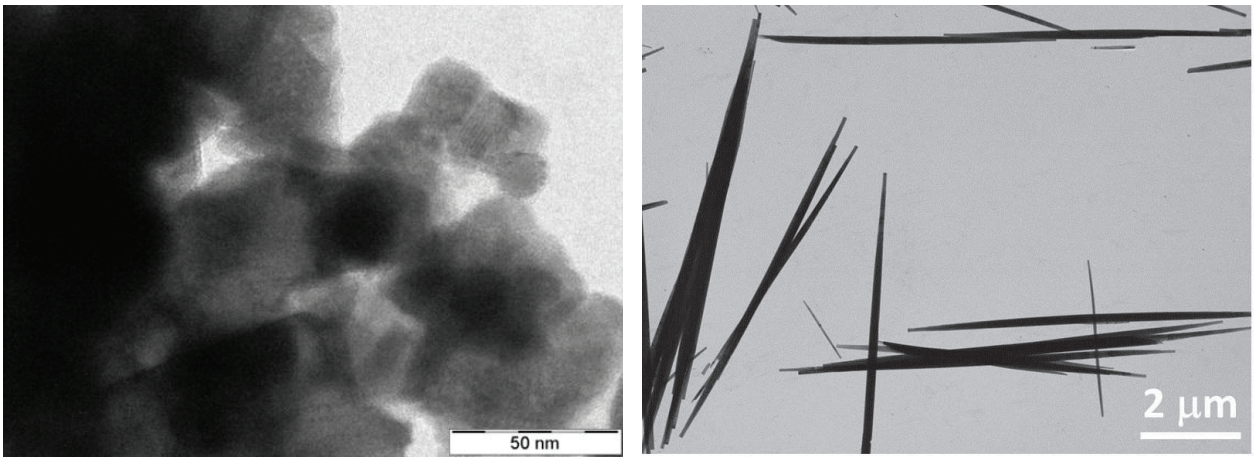

(a) (b)

FIGURE 2. TEM images of h-WO_3 (a) nanoparticles and (b) nanorods.

The hexagonal WO_3 crystalline structure of the nanoparticles and nanorods were confirmed by the XRD study (XRD patterns not shown here). The samples exhibited typical hexagonal WO_3 patterns corresponding to ICDD 85-2460. The results for both the nanoparticles and nanorods indicated that the samples consisted of pure h-WO_3 phases and they were highly crystalline, which was important, as from our previous studies it was determined that WO_3 with higher degree of crystallinity showed better photocatalytic properties [4].

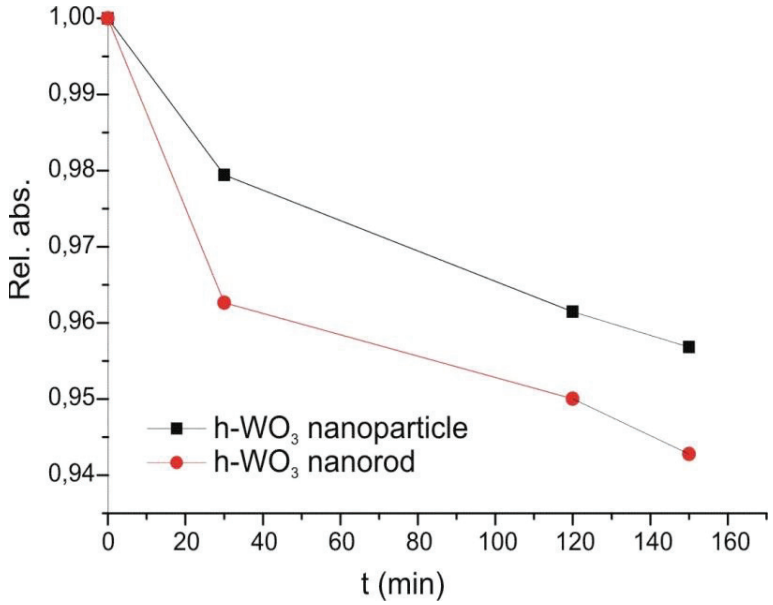

FIGURE 3. Photocatalytic study of h-WO_3 nanoparticles and nanorods: decomposing aqueous methyl orange by UV light.

The photocatalytic activity of the WO_3 powders is shown in Fig. 3. After 150 min reaction time the relative absorbance of methyl orange, which is proportional to its concentration according to Lambert-Beer's law, decreased to 0.96 in the case of using WO_3 nanoparticles as photocatalysts. The WO_3 nanorods performed much better, since in their case the A/A_0 of methyl orange decreased to 0.94. The higher specific surface, i.e. nanorods vs. nanoparticle morphology, is explained as the key factor in the 50 % higher photocatalytic efficiency. The results are still preliminary, and by improving the photocatalytic setup from a cuvette to e.g. a stirred jacketed beaker with much higher volume the A/A_0 decline is expected to be increased significantly, and thus the sensitivity of the photocatalytic measurement will be better. Nevertheless, the obtained data clearly show that h-WO_3 nanorods obtained by hydrothermal synthesis operate much better in photocatalysis than h-WO_3 nanoparticles obtained by thermal decomposition of HATB.

CONCLUSIONS

We obtained h-WO_3 nanoparticles by annealing $(NH_4)_xWO_{3-y}$ in air at 500 °C and h-WO_3 nanorods hydrothermally using Na_2WO_4, HCl, $(COOH)_2$ and $NaSO_4$ as precursors at 200 °C. The h-WO_3 nanoparticles were 50-70 nm in size, while the h-WO_3 nanorods were 150-500 nm thick and 5-10 μm long. Both samples were composed of h-WO_3, without any impurities. The photocatalytic activity of the h-WO_3 nanorods turned out to be 50 % better compared to h-WO_3 nanoparticles, owing to the higher specific surface of the h-WO_3 nanorods.

ACKNOWLEDGMENTS

S. Boyadjiev acknowledges the Postdoctoral Fellowship programme of the Hungarian Academy of Sciences (2013-2015). I. M. S. thanks for a János Bolyai Research Fellowship of the Hungarian Academy of Sciences. An OTKA-PD-109129 grant is acknowledged.

REFERENCES

1. C. Di Valentin, F. Wang and G. Pacchioni, Top. Catal. **56**, 1404–1419 (2013).
2. G. R. Bamwenda and H. Arakawa, Appl. Catal. A **210**, 181–191 (2001).
3. D. Spasiano, R. Marotta, P. Fernández-Ibanes, S. Malato and I. Di Somma, Appl. Catal. B **170–171**, 90–123 (2015).
4. I. M. Szilágyi, B. Fórizs, O. Rosseler, A. Szegedi, P. Németh, P. Király, G. Tárkányi, B. Vajna, K. Varga-Josepovits, K. Lászlo, A. L. Tóth, P. Baranyai and M. Leskelä, J. Catal. **294**, 119–127 (2012).
5. H. Wang, P. Xu and T. Wang, Mater. Des. **23**, 331–336 (2002).
6. G. Xin, W. Guo and T. Ma, Appl. Surf. Sci. **256**, 165–169 (2009).
7. M. Qamar, M. A. Gondal and Z. H. Yamani, Catal. Comm. **10**, 1980–1984 (2009).
8. I. M. Szilágyi, J. Madarász, G. Pokol, I. Sajó, P. Király, G. Tárkányi, A. L. Tóth, A. Szabó and K. Varga-Josepovits, J. Therm. Anal. Calorim. **98**, 707–716 (2009).
9. D. Sánchez-Martínez, A. Martínez-de la Cruz and E. López-Cuéllar, Mat. Res. Bull. **48**, 691–697 (2013).
10. F. A. Ofori, F. A. Sheikh, R. Appiah-Ntiamoah, X. Yang and H. Kim, Nano-Micro Lett. **7**, 291–297 (2015).
11. I. M. Szilágyi, E. Santala, M. Heikkila, V. Pore, M. Kemell, T. Nikitin, G. Teucher, T. Firkala, L. Khriachtchev, M. Rasanen, M. Ritala and M. Leskelä, Chem. Vapor. Dep. **19**, 149–155 (2013).
12. C. Wang, X. Zhang, B. Yuan, Y. Wang, P. Sun, D. Wang, Y. Wei and Y. Liu, Chem. Eng. J. **237**, 29–37 (2014).
13. T. Peng, D. Ke, J. Xiao, L. Wang, J. Hu and L. Zan, J. Sol. State Chem. **194**, 250–256 (2012).
14. D. B. Hernandez-Uresti, D. Sánchez-Martínez, A. Martínez-de la Cruz, S. Sepúlveda-Guzmán and L. M. Torres-Martínez, Ceram. Int. **40**, 4767–4775 (2014).
15. Y. Wicaksana, S. Liu, J. Scott and R. Amal, Molecules **19**, 17747–17762 (2014).
16. A. Phuruangrat, D. J. Ham, S. J. Hong, S. Thongtem and J. S. Lee, J. Mater. Chem. **20**, 1683–1690 (2010).
17. I. M. Szilágyi, F. Hange, J. Madarász and G. Pokol, Eur. J. Inorg. Chem. **17**, 3413–3418 (2006).
18. I. M. Szilágyi, J. Madarász, G. Pokol, P. Király, G. Tárkányi, S. Saukko, J. Mizsei, A. L. Tóth, A. Szabó and K. Varga-Josepovits, Chem. Mater. **20**, 4116–4125 (2008).
19. I. M. Szilágyi, J. Pfeifer, C. Balázsi, A. L. Tóth, K. Varga-Josepovits, J. Madarász and G. Pokol, J. Therm. Anal. Calorim. **94**, 499–505 (2008).